PERGAMON

Journal of Quantitative Spectroscopy & Radiative Transfer 77 (2003) 165–175

Journal of Quantitative Spectroscopy & Radiative Transfer

www.elsevier.com/locate/jqsrt

The reflection function of optically thick weakly absorbing turbid layers: a simple approximation

A.A. Kokhanovsky[a,b,*], V.V. Rozanov[a]

[a] *Institute of Environmental Physics, University of Bremen, P. O. Box 330440, Bremen D-28334, Germany*
[b] *Institute of Physics, Academy of Sciences of Belarus, 70 Skarina Avenue, Minsk 220072, Belarus*

Received 20 March 2002; accepted 22 May 2002

Abstract

The paper is devoted to the derivation of correction terms for the asymptotic formulae of the radiative transfer theory, which allow to increase their accuracy for smaller optical thicknesses (typically, down to the optical thickness equal to 5). Most of the examples are limited to the case of water clouds. However, the main results are easily generalized on other types of disperse media.
© 2002 Published by Elsevier Science Ltd.

Keywords: Radiative transfer; Clouds; Turbid media

1. Introduction

The geometrical thickness L of many natural turbid media is much larger than the mean photon free path length l in the same medium. Clouds, snow, ice, foam, leaves and many other types of light scattering objects belong to this class. This is why the problem of light interaction with optically thick media attracted a lot of attention in the past. Convenient analytical equations for the reflection function of such media were obtained by Germogenova [1]. A specific case of weak absorption by optically thick media was considered by Rozenberg [2] and Zege et al. [3].

It was found [4] that the error of analytical solutions rapidly decreases with the optical thickness $\tau = L/l$, being smaller than 5% for $\tau > 15$ in the case of terrestrial clouds. The error rapidly grows with decrease of the optical thickness. This is due to the fact that in the asymptotic theory [1] terms of order τ^{-n} at $n > 2$ are neglected. The analytical derivation of next terms of the expansion of the reflection function on τ is quite involved.

* Corresponding author. Institute of Environmental Physics, University of Bremen, P.O. Box 330440, Bremen D-28334, Germany. Tel.: +49-421-218-4475; fax: +49-421-218-4555.

E-mail address: alexk@iup.physik.uni-bremen.de (A.A. Kokhanovsky).

0022-4073/02/$ - see front matter © 2002 Published by Elsevier Science Ltd.
PII: S0022-4073(02)00085-7

So the main task of this paper is to introduce empirical correction terms to analytical solutions, which broad the range of their applicability. Cases of nonabsorbing and absorbing media are considered separately.

2. Nonabsorbing media

The reflection function of a nonabsorbing light scattering layer can be obtained from the following analytical equation [1,5–7]:

$$R(\tau,\xi,\eta,\psi) = R^0_\infty(\xi,\eta,\psi) - tK_0(\xi)K_0(\eta), \tag{1}$$

where ξ is the cosine of the light incidence angle ϑ_0, η is the cosine of the observation angle ϑ, ψ is the relative azimuth,

$$t = \frac{1}{\alpha + 0.75\tau(1-g)} \tag{2}$$

is the global transmittance, g is the asymmetry parameter and

$$\alpha = 3\int K_0(\xi)\xi^2\,\mathrm{d}\xi, \tag{3}$$

$$K_0(\eta) = \frac{3}{4\pi}\int_0^{2\pi}\mathrm{d}\psi\int_0^1 R^0_\infty(\xi,\eta,\psi)(\xi+\eta)\xi\,\mathrm{d}\xi. \tag{4}$$

The function $K_0(\eta)$ is called the escape function. It describes the angular distribution of photons, leaving the semi-infinite nonabsorbing scattering layer with light sources located at an infinite depth (the Milne problem). Note, that Eq. (1) can be easily modified to account for a Lambertian underlying surface with the albedo A [5]. We consider here, however, only the case of $A = 0$.

We see that Eq. (1) reduces the calculation of the reflection function of a finite layer for large values of the optical thickness τ to the calculation of the reflection function of a nonabsorbing semi-infinite layer $R^0_\infty(\xi,\eta,\psi)$ with the same phase function as a finite layer under study. A user-friendly code for computing this function is freely available via Internet [8].

The approximate solution for $R^0_\infty(\xi,\eta,\psi)$ at nadir observation was obtained by Kokhanovsky [9]. It has the following simple form:

$$R^0_\infty(\xi,1) = \frac{0.37+1.94\xi}{1+\xi} + \frac{p(\pi - \arccos\xi)}{4(1+\xi)}, \tag{5}$$

where $p(\theta)$ is the phase function and θ is the scattering angle. It does not depend on the azimuth due to the symmetry of the problem. The approximate formula for the escape function is given by Sobolev [5]:

$$K_0(\xi) = \tfrac{3}{7}(1+2\xi), \tag{6}$$

which gives for α, using Eq. (3): $\alpha \approx 1.07$. The accuracy of Eqs. (5) and (6) is better than 2% at $\xi > 0.2$. Thus, we have a chain of analytical equations (1), (2), (5) and (6), which can be used to calculate the reflection function of a finite optically thick layer at nadir observation. The accuracy of

this approximation is better than 5% at $\xi > 0.2$ and $\tau > 15$. To increase the accuracy of Eq. (1) for smaller values of the optical thickness, we found that an additional correction term in the expression for the transmission t should be added. In particular, we derived, parametrizing the function (see Eq. (1))

$$t^* = \frac{R^0_\infty(\xi,1) - R(\tau,\xi,1)}{K_0(\xi)K_0(1)}, \tag{7}$$

where $R(\tau,\xi,1)$ is obtained with the exact radiative transfer equation solution, that

$$t^* = t - t_c, \tag{8}$$

where

$$t_c = \frac{a - b\xi + c\xi^2}{\tau^3} \tag{9}$$

and $a = 4.86$, $b = 13.08$, and $c = 12.76$. The value $t^* = t - t_c$ should be used in Eq. (1) instead of t, if one likes to increase the accuracy of Eq. (1) for smaller τ. The values of $R^0_\infty(\xi,1)$ and $K_0(\xi)$ in Eq. (7) were obtained from Eqs. (5) and (6). Calculations were performed for a well-known Cloud C1 model of Dermendjian [10] at the wavelength 0.65 μm, where light absorption by water droplets can be neglected. Note, that according to the reciprocity principle it follows from Eq. (9):

$$t_c = \frac{a - b\xi\eta + c\eta^2\xi^2}{\tau^3} \tag{10}$$

at $\eta \neq 1$.

Finally, we have the following expression for the reflection function at nadir observation, which follows from Eqs. (1), (2), (5), (6), and (8):

$$R(\tau,\xi,1) = \frac{0.37 + 1.94\xi}{1+\xi} + \frac{p(\pi - \arccos\xi)}{4(1+\xi)} - \frac{27}{49}\left(\frac{1}{1.07 + 0.75\tau(1-g)} - t_c\right)(1+2\xi). \tag{11}$$

This equation reduces the calculation of the reflection function at nadir observation to that of the phase function calculation. Note, that the second term, containing the phase function, is smaller that the first one and can be often neglected (especially for rapid estimations).

We study the accuracy of Eq. (11) in Figs. 1–3 for various values of optical thicknesses, effective radii of water droplets and incidence angles. The particle size distribution is given by

$$f(a) = Ba^6 \exp(-9a/a_{ef}), \tag{12}$$

where B is the normalization constant. The wavelength is equal to 0.65 μm.

In particular, the dependence of the reflection function on the solar angle is presented in Fig. 1 for various values of the cloud optical thickness τ and the effective radius of droplets a_{ef}. We see that Eq. (11) describes all important silent features of backscattered light. Namely, rainbow and glory phenomena present at solar angles around 40 and 0 degrees (scattering angles 140° and 180°, respectively). The rainbow is enhanced for the largest particles in Fig. 1. The minimum in glory scattering occurs for smaller scattering angles for smaller particles than it is for larger particles. The reflection function takes values from 0.1 till 1.1 in Fig. 1, while τ increases from 5 to 100, which

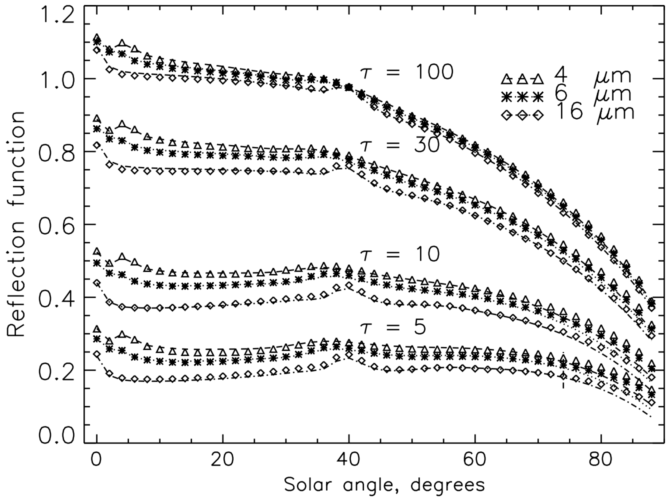

Fig. 1. The dependence of the reflection function of a plane–parallel homogeneous cloud layer with water droplets on the solar angle at nadir observation for different values of the cloud optical thickness, the effective radius of droplets and the wavelength 0.65 μm (exact data—symbols, approximation (11)—lines). The droplet size distribution is given by Eq. (12).

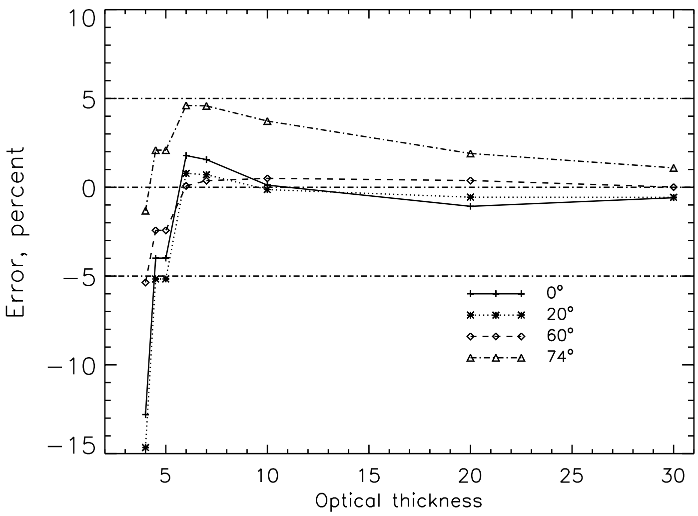

Fig. 2. The error of approximation (11) as a function of the optical thickness for various solar angles and $a_{ef} = 6$ μm. Other parameters as in Fig. 1.

is a standard range of optical thicknesses for terrestrial water clouds. The approximation works well (see also Figs. 2 and 3) both for highly reflecting clouds and clouds with low reflection ($R \sim 0.2$).

Note, that the dependence of the reflection function on the effective radius is more strong for smaller optical thicknesses, where single scattering still plays an important role. This dependence is almost disappeared for semi-infinite media due to highly developed multiple light scattering [9]. The glory scattering region is the most sensitive to the size of droplets. For instance, the reflection

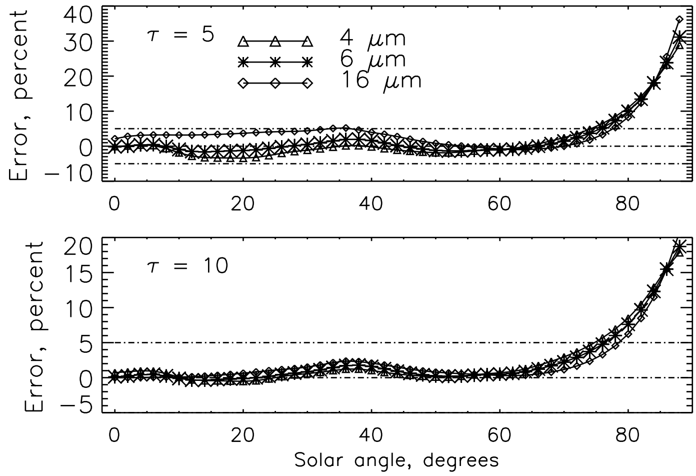

Fig. 3. The error of approximation (11) as a function of the solar angle for various values of the effective radius and $\tau = 5, 10$. Other parameters as in Fig. 1.

function can differ more by 50% for values of $a_{\mathrm{ef}} = 4$ μm as compared to the case of $a_{\mathrm{ef}} = 16$ μm (see the case of $\tau = 5$) at small solar zenith angles. The difference, however, is smaller than 10% at $\tau = 100$ (see Fig. 1).

Relative errors of Eq. (11) are given in Fig. 2 for different solar angles as the function of the optical thickness and $a_{\mathrm{ef}} = 6$ μm. They are smaller than 5%. The error is smallest at an incidence angle of 60°. The dependence of errors of the approximation on the size of droplets is presented in Fig. 3 as the function of the solar angle for optical thicknesses 5 and 10, where the largest error of the approximation is expected, and various values of the effective radius of water droplets, characteristic for water clouds, ranging from 4 to 16 μm. Almost in all cases the error is smaller than 5%. It only weakly depends on the size of droplets. The errors are larger for Sun at the horizon (solar zenith angle is larger than 75°). However, this case cannot be treated in the framework of the plane—parallel geometry anyway.

Summing up, the error of simple Eq. (11) is better than 5% at $\tau \geqslant 5$, $\vartheta_0 < 75^\circ$ and $a_{\mathrm{ef}} = 4$–16 μm for the case of water droplets. Thus, Eq. (11) can be used in a number of applications, including optical thickness determination from reflection function measurements.

It should be pointed out that the reflection function of clouds is often used to their optical thickness determination [11], assuming a priori value of the effective radius of droplets. To study the influence of the deviation of the reflection function of clouds with droplet size distributions, having $a_{\mathrm{ef}} = 16$ and 4 μm from that for the case of $a_{\mathrm{ef}} = 6$ μm, we have presented the differences

$$\Delta_1 = \frac{R(a_{\mathrm{ef}} = 6\ \mu\mathrm{m}) - R(a_{\mathrm{ef}} = 16\ \mu\mathrm{m})}{R(a_{\mathrm{ef}} = 6\ \mu\mathrm{m})}, \qquad \Delta_2 = \frac{R(a_{\mathrm{ef}} = 6\ \mu\mathrm{m}) - R(a_{\mathrm{ef}} = 4\ \mu\mathrm{m})}{R(a_{\mathrm{ef}} = 6\ \mu\mathrm{m})} \tag{13}$$

in Fig. 4. Calculations were performed for a nadir observation. We see that these differences are in the range [−45%, 15%], depending on the size of droplets and the incidence angle. This can influence considerably the optical thickness retrieval. Thus, actual values of a_{ef} cannot be neglected in the cloud optical thickness retrieval algorithms. It follows from Eq. (11) that the dependence

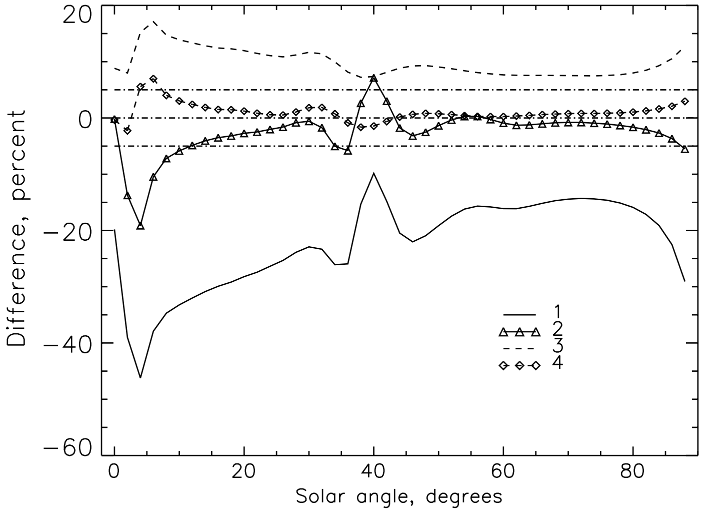

Fig. 4. The differences $\Delta_1(1,2)$, $\Delta_2(3,4)$ (see Eqs. (13)) as functions of the solar angle. Other parameters as in Fig. 1. The values $\Delta_1(2)$ and $\Delta_1(4)$ correspond to the case of adjusted asymmetry parameters as described in the text.

of the reflection function on the effective radius is determined by two separate factors, namely the phase function and the asymmetry parameter. To separate these dependencies, we present in Fig. 4 also differences (13), assuming that the asymmetry parameter is correct and corresponds to the case of particle size distributions with $a_{\rm ef} = 16$ and 4 μm, respectively (see Eq. (11)), but the phase function corresponds to the case of droplets with $a_{\rm ef} = 6$ μm both for $R(a_{\rm ef} = 16$ and 4 μm). Then the differences are much smaller. They are within 5% for almost all solar angles (with exception of glory scattering, where it could reach 20%, see Fig. 4). This makes it possible to use the same phase function in the satellite cloud optical thickness retrieval. However, the value of g should be adjusted to the actual value of the effective radius of droplets, which can be obtained from measurements in the infra-red region of the electromagnetic spectrum.

3. Weakly absorbing media

The analytical result for the reflection function of weakly absorbing light scattering media was obtained by Rozenberg [2]. Namely, we have

$$R(\tau,\xi,\eta,\psi) = R_\infty(\xi,\eta,\psi) - T\exp(-y-x)K(\xi)K(\eta), \tag{14}$$

where

$$T = \frac{sh(y)}{sh(x+y)} \tag{15}$$

is the global transmittance of a weakly absorbing layer and $x = \sqrt{3(1-g)\beta}\tau$, $y = 4\sqrt{\beta/3(1-g)}$. The value of β gives the probability of absorption in a light scattering event.

It should be stressed that Eq. (14) should transform to Eq. (1) as $\beta = 0$. This is not the case, however. We have from Eq. (15) at $\beta = 0$:

$$T = \frac{1}{1 + 0.75(1-g)\tau}, \tag{16}$$

which differs from Eq. (2).

Eq. (2) was derived from the asymptotical analysis of the radiative transfer equation. In derivation of Eq. (15) some phenomenological assumptions were made. This explains the difference. We propose to modify y in the denominator of Eq. (15) to make it consistent with Eq. (2). Then we have instead of Eq. (15)

$$T = \frac{sh(y)}{sh(x + \alpha y)}. \tag{17}$$

Eqs. (17) transforms to Eq. (2) as $\beta = 0$. Moreover, we introduce the correction term (10) in Eq. (14). Then we have finally

$$R(\tau, \xi, \eta, \psi) = R_\infty(\xi, \eta, \psi) - \left(\frac{sh(y)\exp(-x)}{sh(x + \alpha y)} - t_c \right) \exp(-y) K_0(\xi) K_0(\eta), \tag{18}$$

where we also neglected the influence of the absorption on the escape functions. Eq. (18) reduces the calculation of the reflection function of a finite absorbing layer to that of a semi-infinite absorbing layer $R_\infty(\xi, \eta, \psi)$. Note, that due to the relation [3]

$$R_\infty(\xi, \eta, \psi) = R^0_\infty(\xi, \eta, \psi) \exp(-uy), \tag{19}$$

where

$$u = \frac{K_0(\xi) K_0(\eta)}{R^0_\infty(\xi, \eta, \psi)}, \tag{20}$$

the initial problem is reduced to the calculation of the reflection function of a semi-infinite nonabsorbing layer. We found, using exact calculations, that the accuracy of Eq. (19) can be improved for larger β, modifying u in Eq. (19). Namely, one should use the parameter

$$u^* = (1 - 0.05y)u, \tag{21}$$

instead of u in Eq. (19).

The accuracy of Eq. (18) in account with Eqs. (19)–(21), (5) and (6) is presented in Figs. 5–7 for the case of the nadir observation at $\lambda = 1.55$ μm and different τ and a_{ef}.

In particular, the cloud reflection function at the nadir observation is given in Fig. 5 for different cloud optical thicknesses and $a_{ef} = 6$ μm. Both approximate results, obtained with Eq. (18), and the exact data are presented. The reflection function increases with the optical thickness, which corresponds to the dependence of the reflection function on the optical thickness is visible, where clouds do not absorb (see Fig. 1).

Comparing Figs. 1 and 5, we see that the reflection function for absorbing clouds is smaller than for nonabsorbing clouds at $\tau = 100$. This is not the case for smaller optical thicknesses (see, e.g., cases of $\tau = 5$ in Figs. 1 and 5). Such a behaviour can be understood taking into account that Figs. 1 and 5 are prepared at different wavelengths. This results in different effective diffraction parameters, phase functions and asymmetry parameters for cases, presented in Figs. 1 and 5. In particular, the

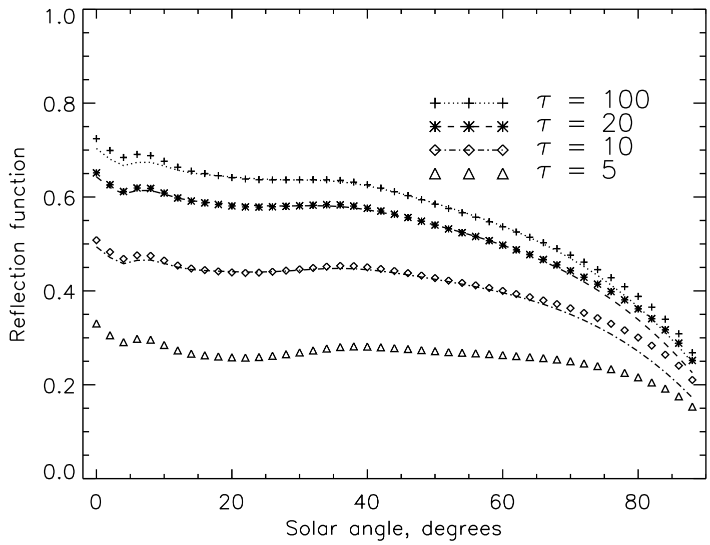

Fig. 5. The dependence of the reflection function of a plane-parallel homogeneous cloud layer with water droplets on the solar angle at nadir observation for different values of the cloud optical thickness at the effective radius of droplets equal to 6 μm, the wavelength equal to 1.55 μm (exact data—symbols, approximation (18)—lines). The droplet size distribution is given by Eq. (12).

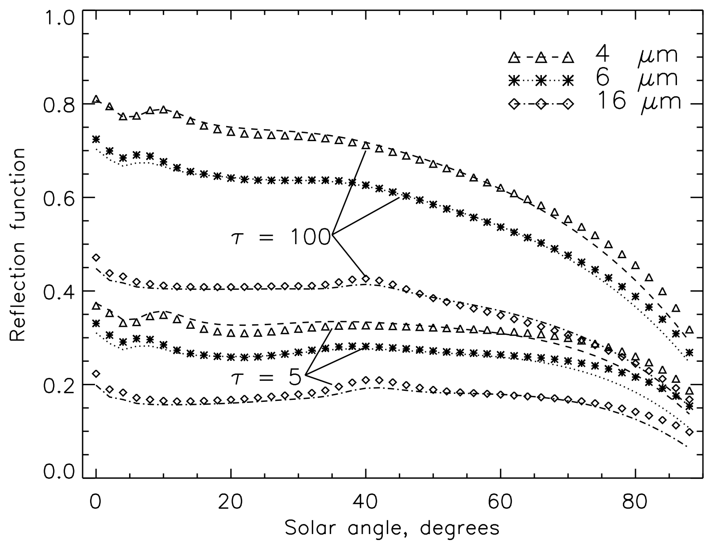

Fig. 6. The same as in Fig. 5 but for various effective radii and $\tau = 5, 100$.

effective diffraction parameter of droplets $2\pi a_{ef}/\lambda$ is smaller at $\lambda = 1.55$ μm (see Fig. 5) as compared to the case of $\lambda = 0.65$ μm (see Fig. 1). Also the asymmetry parameter and, correspondingly, the light transmission at a given optical thickness and no absorption is also somewhat smaller at $\lambda = 1.55$ μm. This results in larger reflection for smaller particles, which is also confirmed by Fig. 1. Thus, almost

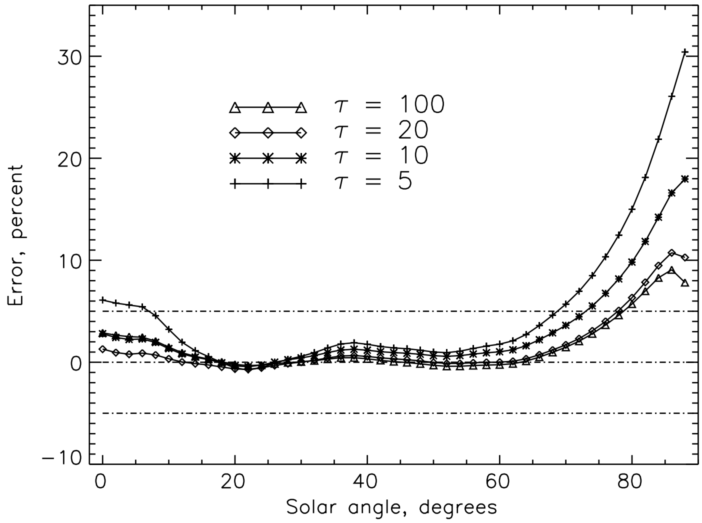

Fig. 7. The error of approximation (18), obtained using data in Fig. 5.

the same values of the reflection function in Fig. 5 at $\tau = 5$ as compared to data in Fig. 1 at $\tau = 5$ are due to two factors, namely—the decrease of R due to absorption and increase of R due to the effect of the effective diffraction parameter of droplets. These two processes almost compensate each other in the case under study.

The reflection function of a water cloud at nadir observation and various thicknesses of clouds and effective sizes of droplets is given in Fig. 6 as a function of a zenith solar angle. It follows from Fig. 6 that the reflection function of a cloud with the optical thickness of 100 and the size of droplets 16 μm is close to the reflection function of the cloud with the optical thickness 5, but for the effective radius 4 μm. This shows the importance the size of droplets for the reflection function calculation in the near-infrared as compared to the case of the visible part of the spectrum, considered in the previous section. It follows (see Fig. 7) that the error of Eq. (18) is smaller than 5% at the wavelength 1.55 μm and incidence angles smaller than 75°. Thus, this equation together with Eq. (11) can be used as a base of a semi-analytical algorithm for the size of particles and optical thickness retrieval from reflection function measurements at wavelengths 0.65 and 1.55 μm.

The complex refractive index of water at 1.55 μm is 1.3109-0.0001348i and, therefore, the probability of photon absorption β is quite small. It is equal to 0.0065 at $a_{\rm ef} = 6$ μm, for example (with $g = 0.8214$). It is interesting to study the influence of β on the error of the approximation (18). For this, we have calculated the phase functions (and also values of g and β, see Table 1) with the Mie theory, using the particle size distribution (12) at $a_{\rm ef} = 6$ μm and the refractive index $m = 1.3109 - {\rm i}\chi$, where χ was taken equal to 0.00001, 0.00005, 0.0001, 0.0005, and 0.001. These calculated local optical characteristics then were used to find the reflection function both with the approximate theory and the exact radiative transfer code. We found (see Fig. 8) that for $\beta < 0.0024$ the error of the approximation is better than 5% for incidence angles smaller 75° and nadir observation. The error is equal to 5% also at $\beta < 0.035 (y < 1.2)$, but for smaller range of incidence angles $15^\circ < \vartheta_0 < 65^\circ$, which are quite typical for satellite observations. It amounts to approximately 15% for the case of the solar angle in nadir and $\chi = 0.001$. It should be pointed out that the value of $\chi = 0.0005$ for water

Table 1
The dependence of β, g, y on χ

χ	β	g	y
0.00001	0.0005	0.8199	0.12
0.00005	0.0034	0.8204	0.27
0.00010	0.0047	0.8210	0.37
0.00050	0.0226	0.8253	0.83
0.00100	0.0435	0.8300	1.20

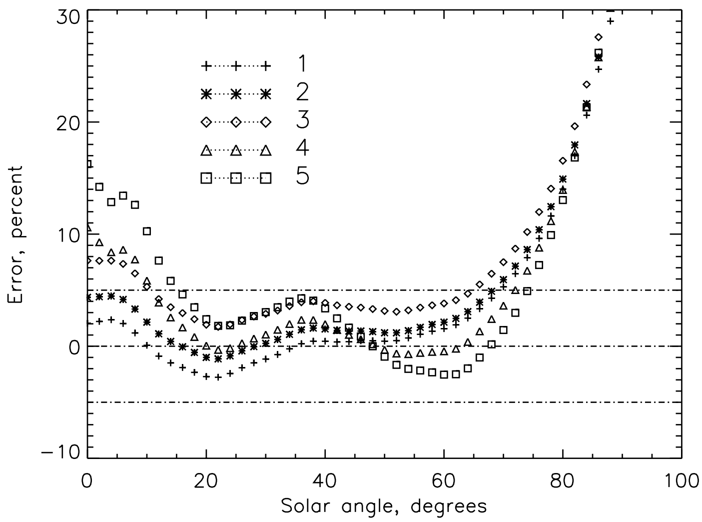

Fig. 8. The error of approximation (18) for various values of $y = 0.12(1), 0.27(2), 0.37(3), 0.83(4)$, and $1.2(5)$ (see also Table 1).

corresponds approximately to the wavelength 2.312 μm. This allows to use equations presented here for the case of water clouds both in visible and near-infrared. This range of wavelength is often used for the estimation of cloud properties from space.

4. Conclusion

We have proposed here modified equations for the calculation of the reflection function of optically thick media, which reduces the calculation of reflection function of weakly absorbing scattering layers to the calculation of the reflection function of a nonabsorbing semi-infinite layer. The code to calculate the reflection function of a semi-infinite layer is freely available via Internet [8]. At nadir observation the problem is reduced to the calculation of the phase function. Note, that the values of the phase function are usually small numbers in the backward hemisphere. Then the second term in Eq. (5) can be neglected as compared to the first one. This implies that we have an analytical equation for the reflection function at the nadir observation for incidence angles smaller than 75°. This analytical solution can be used, e.g., for the characterization of light scattering, absorption and

microphysical parameters of turbid media from spectral measurements of the reflection function. Our study was restricted to the case of water clouds. However, results with slight modification can be used for other light scattering media. The accuracy of analytical solutions obtained is better than 5% at solar angles less than 75° and nadir observation.

Acknowledgements

This work was supported by the Institute of Environmental Physics (University of Bremen).

References

[1] Germogenova TA. On the nature of the transport equation solution for a plane-parallel layer. Zh. Vychisl. Mat. i Mat. Fiz. 1961;1(6):1001–19.
[2] Rozenberg GV. Optical characteristics of thick weakly absorbing scattering layers. Dokl. AN SSSR 1962;145:775–7.
[3] Zege EP, Ivanov AP, Katsev IL. Image transfer through a scattering medium. New York: Springer, 1991.
[4] Minin IN. Radiative transfer theory in planetary atmospheres. Moscow: Nauka, 1988.
[5] Sobolev VV. Light scattering in planetary atmospheres. Moscow: Nauka, 1972.
[6] Van de Hulst HC. Multiple light scattering: tables, formulas and applications. New York: Academic Press, 1980.
[7] Kokhanovsky AA. Light scattering media optics: problems and solutions. Chichester: Springer-Praxis, 2001.
[8] Mishchenko MI, Dlugach JM, Yanovitskij EG, Zakharova NT. Bidirectional reflectance of flat, optically thick particulate layers: an efficient radiative transfer solution and applications to snow and soil surfaces, JQSRT 1999;63:409–32.
[9] Kokhanovsky AA. Simple approximate formula for the reflection function of a homogeneous, semi-infinite turbid medium, J Opt Soc Am 2002;19:957–60.
[10] Dermendjian D. Light scattering by spherical polydispersions. Amsterdam: Elsevier, 1969.
[11] Rossow WB. Measuring cloud properties from space: a review, J Climate 1989;2:419–58.